

# Classification of Images of Childhood Pneumonia using Convolutional Neural Networks

A. A. Saraiva<sup>1</sup> <sup>a</sup>, N. M. Fonseca Ferreira<sup>2,3,4</sup> <sup>b</sup>, Luciano Lopes de Sousa<sup>5</sup> <sup>c</sup>,  
Nator Junior C. Costa<sup>5</sup> <sup>d</sup>, José Vigno Moura Sousa<sup>5,6</sup> <sup>e</sup>, D. B. S. Santos<sup>5</sup> <sup>f</sup>, Antonio Valente<sup>2,7</sup>  
<sup>g</sup> and Salviano Soares<sup>7</sup> <sup>h</sup>

<sup>1</sup>UTAD University, Coimbra, Portugal

<sup>2</sup>INESC-TEC Technology and Science, Campus da FEUP, Rua Dr. Roberto Frias 378, 4200 - 465 Porto, Portugal

<sup>3</sup>Knowledge Engineering and Decision-Support Research Center (GECAD) of the Institute of Engineering,  
Polytechnic Institute of Porto, Portugal

<sup>4</sup>Department of Electrical Engineering, Institute of Engineering of Coimbra, Polytechnic Institute,  
Rua Pedro Nunes, 3031-601 Coimbra, Portugal

<sup>5</sup>State University of Piauí, Piauí, Brazil

<sup>6</sup>University Brazil, São Paulo, Brazil

<sup>7</sup>IEETA-UA and School of Science and Technology, University of Trás-os-Montes and Alto Douro, Vila Real, Portugal

Keywords: Pneumonia, X-Ray, CNN, K-Fold.

**Abstract:** In this paper we describe a comparative classification of Pneumonia using Convolution Neural Network. The database used was the dataset *Labeled Optical Coherence Tomography (OCT) and Chest X-Ray Images for Classification* made available by (Kermany, 2018) with a total of 5863 images, with 2 classes: normal and pneumonia. To evaluate the generalization capacity of the models, cross-validation of k-fold was used. The classification models proved to be efficient compared to the work of (Kermany et al., 2018) which obtained 92.8 % and the present work had an average accuracy of 95.30 %.

## 1 INTRODUCTION

Pneumonia is one of the most common causes of death in children worldwide, accounting for 15 % of all deaths of children under 5 years of age (Mathur et al., 2018). Identifying and treating pneumonia has a substantial effect on infant mortality. Although methods utilizing chest X-ray are promising modalities for radiologic diagnosis, their role in clinical management and their impact on outcomes need to be improved (Zar et al., 2017).

For an adequate treatment, therefore, an early diagnosis of pneumonia is necessary, but it is not always clear (Saraiva et al., 2018a), (Saraiva et al., 2018e). In a review of the medical records of patients admitted with pneumonia, 22 % of the patients presented some reason for the uncertainty of the diagnosis, which could result in delays in the delivery of antibiotics. Furthermore, chest computed tomography is a gold standard for diagnosis, but it is not always available and is loaded with a high dose of radiation and high cost, preventing its use in the routine diagnostic process of patients with suspected pneumonia (Cortellaro et al., 2012) (Saraiva et al., 2018f), (Marques et al., 2018), (Saraiva et al., 2018c).

Several researchers use imaging for the detection of pneumonia. Most methods use radiographic imaging as a tool. For example, in (Sharma et al., 2017), to detect clouds of pneumonia, the Otsu threshold was used, which will separate the healthy part of the lung from the nebulous regions infected by pneumo-

<sup>a</sup>  <https://orcid.org/0000-0002-3960-697X>  
<sup>b</sup>  <https://orcid.org/0000-0002-2204-6339>  
<sup>c</sup>  <https://orcid.org/0000-0003-0551-4804>  
<sup>d</sup>  <https://orcid.org/0000-0001-5636-424X>  
<sup>e</sup>  <https://orcid.org/0000-0002-5164-360X>  
<sup>f</sup>  <https://orcid.org/0000-0003-4018-242X>  
<sup>g</sup>  <https://orcid.org/0000-0002-5798-1298>  
<sup>h</sup>  <https://orcid.org/0000-0001-5862-5706>

nia, and a detection method based on neural networks using tomography models computerized, was used in (Rajaraman et al., 2018). In addition to these methods, there are projects that extract information from the cough sound analysis to diagnose cases of pneumonia (Amrulloh et al., 2018).

The doctor, when interpreting the chest x-ray, will look for white patches in the lungs to detect pneumonia. However, such hazy patterns would also be observed tuberculosis and severe cases of bronchitis. For the purpose of conclusive diagnosis, the purpose of this study is to identify pneumonia, through analysis of chest X-ray images, to recognize patterns of the disease using a neural network.

The classification stage consists of two sub-steps, where the first one is the training of a Convolutional Neural Networks (CNN), the second one is the validation of the model, that is, the test with images not known by CNN. The method covered ensures a robust coverage in image recognition (Saraiva et al., 2018d), (Saraiva et al., 2018g) (Saraiva et al., 2018b), under certain assumptions that will be clarified throughout the text. A classification model (CNN) for the pneumonia and normal classes is proposed. The results are compared with the work of (Kermany et al., 2018) and obtained a slightly higher result, and the present work presents cross-validation of k-fold. In order to strengthen the results.

This article is divided into 5 sections, and section 2 is intended for related works. In section 3, it is composed by the methodology, where will be explained the steps taken for the development of the algorithm. In section 4, it is assigned to the results obtained and, following in the next section, in 5, where the conclusion of the work is presented.

## 2 RELATED WORK

For the detection of pulmonary diseases chest radiography is always required to identify pulmonary problems. Diseases such as tuberculosis, pneumonia and lung cancer are a major threat to human health. Thus, in (Khobragade et al., 2016) proposes pulmonary segmentation, extraction of characteristics and its classification using an artificial neural network for the detection of pulmonary diseases. (Khobragade et al., 2016) a simple image processing technique with intensity based method was used, and a method based on the discontinuity to detect pulmonary limits, in this way, statistical and geometric characteristics were extracted. Neural networks were used feed forward and back propagation to detect diseases.

Pneumonia is one of the leading causes of infant

mortality. In developing countries there is little infrastructure and doctors in rural areas to provide the necessary diagnosis. Therefore, in (Barrientos et al., 2016) proposes a method for automatic diagnosis using ultrasonography of the lungs. The approach presented is based on the analysis of patterns in rectangular segments in the image of the ultrasonography. The specific characteristics and characteristic vectors were obtained and classified by a standard neural network. In (Barrientos et al., 2016) I obtained a sensitivity of 91.5 % and specificity of 100 % but were extracted from a single patient and only included in the test or in the training set.

Many researchers have developed several algorithms for the diagnosis of lung diseases through sound. One of the parameters used for the detection of pulmonary sound is entropy, so there are differences in the sound of a normal respiratory system and a system with pathologies. In the article (Rizal et al., 2017) discourses several measures of entropy for a classification of pulmonary sounds. The result in (Rizal et al., 2017) shows that the use of a single entropy could not achieve high accuracy, so 7 entropies were used and guaranteed 94.95 % accuracy using multilayer perceptron.

In paper (Rodrigues et al., 2018) suggests a Structural Co-occurrence Matrix (SCM) approach to classify malignant nodules or benign nodules and also their level of malignancy. The structural co-occurrence matrix technique was applied to extract characteristics of the nodule images and classify them. The SCM was applied in gray scale and images of the Hounsfield unit with four filters, creating eight different configurations. The classification stage used classifiers known as the multilayer perceptron, support vector machine, k-Nearest Neighbors algorithm and were applied in two tasks: (i) to classify the nodule images as malignant or benign, (ii) to classify the nodules pulmonary lesions at the level of malignancy (1 to 5). O (Rodrigues et al., 2018) had a result of 96.7 % for precision and F-score measurements in the first task and 74.5 % accuracy and 53.2 % F-score in the second task.

The (Santosh and Antani, 2018) has proposed an idea that takes into account the alterations of the right and left lung region in terms of symmetry and automated the chest X-ray system for the evidence of tuberculosis. The proposed method is the observation of radiological exams leading to bilateral comparisons in the lung field. In (Santosh and Antani, 2018) analyzed the symmetric lung region using a multiple-scale shape feature, as well as border texture characteristics. Three different types of classifiers were used: Bayesian network, multilayer network percep-

tron and random forest. The results obtained with an abnormality detection accuracy of 91 % and area under the ROC curve of 0.96.

Many researchers use various methods for detecting diseases based on lung sound, for example the use of entropy measurement. Sound of pulmonary snoring is a sound that is discontinuous, of short duration and appears in the inspiratory, expiratory or in both cases. Thus, in (Rizal et al., 2016) the Tsallis entropy was used as the characteristic extraction method to classify lung sounds. The results were achieved using at least three Tsallis entropy values with  $q = 2, 3$ , and 4 with MLP as a classifier and three-fold cross validation at an accuracy of 95.35 %, sensitivity of 90.48 % and 100 % specificity, were achieved.

Lung cancer accounts for 26 % of all cancer deaths in 2017, accounting for more than 1.5 million deaths. Thus, in (d. Nóbrega et al., 2018) is proposed to explore the performance of deep transfer learning to classify pulmonary nodule malignancies. In this work, we have used a convolutional neural network such as VGG16, VGG19, MobileNet, Xception, InceptionV3, ResNet50, Inception-ResNet-V2, DenseNet169, DenseNet201, NASNetMobile and NASNetLarge, where they were used to extract parameters from an image database of the lung. The characteristics were classified using Naive Bayes, Perceptron multilayer, support vector machine, Near Neighbors and Random Forest. The results obtained in (d. Nóbrega et al., 2018) were 88.41 % of ACC and 93.19 % of AUC.

(Paing and Choomchuay, 2017) has the objective of detecting pulmonary nodules from a series of digitized CT images. The threshold and morphological operations of Otsu are applied for the segmentation of nodules. In (Paing and Choomchuay, 2017), after segmentation, objects that can not be nodes are discarded. In view of this, multilayer Perceptron was used for the classification and 95 % accuracy was achieved.

In the work (Kermany et al., 2018) a method was proposed using Convolutional Neural Networks with a transfer learning technique. Transfer learning has proven to be a highly effective technique, particularly when confronted in domains with limited data. The main application of the transfer learning algorithm was in the diagnosis of OCT images of the retina, but it was also tested in pediatric thoracic radiographs. In case of retinal OCT, in a multiclass comparison between choroidal neovascularization, diabetic macular edema, drusen and normal, obtained a precision of 96.6 %, with a sensitivity of 97.8 %, a specificity of 97.4 %. In the comparison of chest X-rays with pneumonia versus normal, it obtained an accuracy of 92.8

%, with sensitivity of 93.2 % and specificity of 90.1 %.

The convolutional neural networks offer great help in detecting diseases such as (Lisowska et al., 2017), (Ponzio et al., 2018) and (Mabaso et al., 2018). Therefore, a 3D Convolutional Neural Network for the detection of subtle signs of a Stroke has been proposed in (Lisowska et al., 2017), thus, the architecture was developed to explore contralateral resources and anatomical information from the cerebral atlas. In the work (Ponzio et al., 2018), a deep learning technique based on Convolutional Neural Networks was proposed to differentiate adenocarcinomas from healthy tissues and benign lesions. In the article (Mabaso et al., 2018), it presents an automated way of detecting and counting points in microscopic images based on a Convolutional Neural Network based on a sliding window for detection of multiple points in microscopic images.

Before these works, in this one, the objective is the construction of an algorithm that recognizes the pneumonia, from x-ray images of the thoracic region. In the algorithm, a Convolutional Neural Network was used to recognize patterns in the images of people infected by pneumonia, either by virus or bacteria.

### 3 METODOLOGY

#### 3.1 Description of the Dataset

In the dataset (Kermany, 2018) used for training and validation, it contained 5863 X-ray (JPEG) images and two categories: Normal and Pneumonia. A total of 5863 patients (Junge and Dettori, 2018)

The radiographic images were from pediatric patients one to five years old from the Medical Center in Guangzhou. In this way, radiographs were performed as part of clinical care.

All images in dataset (Kermany, 2018) underwent a treatment in order to remove all low-quality scans, as well as being classified by two specialist physicians and by a third party specialist, in order to prevent any misclassification.

##### 3.1.1 Pneumonia (Bacterial and Viral) and Normal

For the diagnosis of pneumonia, the alveoli become filled with secretion and appear as a white spot on the chest radiograph. Pulmonary consolidation means that the pulmonary alveoli are filled with inflammatory fluid. In radiography, pulmonary consolidation corresponds to an opacity, that is, the whitish area. As

shown in the Figure 1 (II), the X-ray of the thoracic region of patients presenting with pneumonia and X-ray of patients under normal conditions, shown in Figure 1 (I).

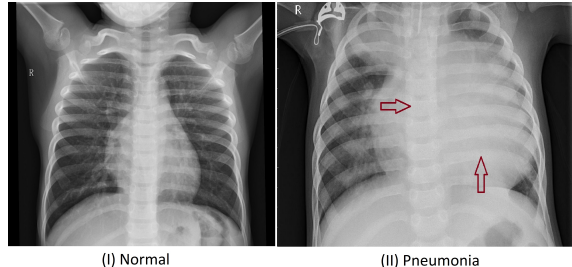


Figure 1: Exemple normal and pneumonia.

### 3.2 Input Structure for Learning Model

In Figure 2 the classification structure is represented, which consists of the image entry in the network, responsible for classification in pneumonia or normal. Images are converted to grayscale and normalized so that they are between 0 and 1, making them a 32-bit floating point.

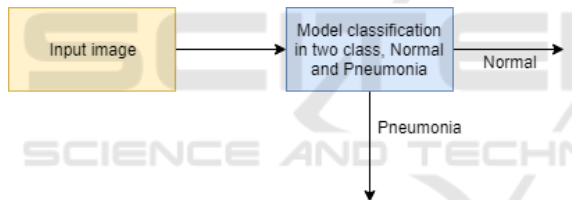


Figure 2: Exemple input image.

### 3.3 Training Structure

The training and validation structure has three steps, represented in Figure 3, the first one is the division and normalization of the images. In the second one the training of the images is realized. Network validation is performed using the test data.

To validate the model, cross-validation of k-fold is used, which consists of dividing the images into two sets: test and training. The process is repeated 5 times, changing the test and training images after the calculation of k.

### 3.4 Proposed Model Convolution Neural Network (CNN)

In the first stage we have the convolutional layer, which is one of the main layers, where it is the extraction of characteristics of the image through a series of

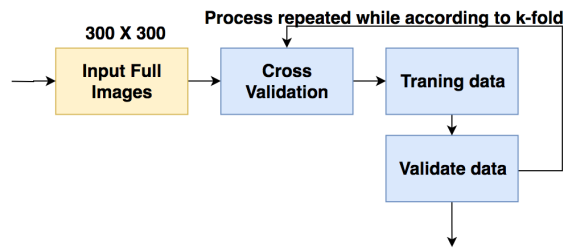


Figure 3: Training structure and validation.

filters (kernels). A filter is an array of values, called weights, trained to detect specific features. The filter moves over each part of the image to see if the feature that it should detect is present. When the feature is present in part of an image, the convolution operation between the filter and that part of the image results in a real number with a high value. If the resource is not present, the resulting value will be low. To provide a value that represents the confidence that a particular resource is present, the filter performs a convolution operation, which is an elementary product and sums between two arrays.

Given a two-dimensional image,  $I$ , and a small array,  $K$  of size  $h \times w$  (kernel), the convoked image,  $I * K$ , is calculated by superimposing the kernel at the top of the image all possible forms, and recording the sum of the elementary products between the image and the kernel equation 1.

$$(I * K)_{xy} = \sum_{i=1}^h \sum_{j=1}^w K_{ij} \cdot I_{x+i-1, y+j-1} \quad (1)$$

After the convolution layer is the pooling layer, which is responsible for reducing the spatial size of the feature map, preserving the resources detected in a smaller representation. There are several pooling layer options, with maxpooling being the most popular. Basically, maxpooling operates by locating the locations in the image that show the strongest correlation for each resource (the maximum value) are preserved and those maximum values combine to

1	0	0	2	3	2	5	1
3	2	1	0	4	5	3	2
2	4	1	4	0	2	3	1
4	5	0	8	4	6	0	4
0	2	7	2	0	0	1	2
1	3	9	0	1	1	3	3
7	2	2	4	1	3	0	1
1	3	9	2	2	0	4	2

Figure 4: Example max-pooling with a 8x8 image.

form a smaller space as shown in Figure 4. In general, they are used after the convolutional layers, both with the objective of progressively reducing computational costs in the network, as well as minimizing the probability of overfitting.

After the pooling layer, we find the fully connected layers (FCN) that are used to make final predictions. A FCN layer obtains "resources" in a vector form from a previous resource extraction layer, multiplies a weight matrix, and generates a new resource vector whose computation pattern is a dense matrix-vector multiplication (Zhang et al., 2018). Some FCNs are used in a cascade mode that ultimately produce the CNN classification result that generates a probability (a number ranging from 0 to 1) for each of the classification labels that the model is trying to predict. Sometimes multiple input vectors are processed simultaneously in a single batch to increase the overall throughput as shown in the following expression when the batch size  $h$  is greater than 1. Note that the FCN layers are also the major components of neural networks (DNNs) that are widely used in speech recognition (Zhang et al., 2018).

$$Out[m][h] = \sum_{n=0}^N W[m][n] * In[n][h] \quad (2)$$

### 3.4.1 Categorical Cross-entropy

The cross-entropy loss measures the performance of a classification model, with the output being a probability value ranging from 0 to 1 (Zhang and Sabuncu, 2018).

$$H(p, q) = - \sum_x p(x) \log q(x). \quad (3)$$

### 3.4.2 CNN Architecture

In Figure 5 is the CNN architecture used, it has 10 layers, the first seven convolutionals and the last three without convolution with the softmax activation function (Peng et al., 2017) equation 4, the network input receives a 300x300 pixel image, each convolution layer has the ReLUs enable function. For the convolution kernel, the 3x3 size was adopted, because this way it is possible to have a greater precision in the time to go through the entire image.

After two convolutional layers a Max-pooling layer is used, this reduces the size of the matrices resulting from the convolution. With this layer it is possible to reduce the amount of parameters that will be learned by the network, this way it is done overfitting control.

In the last layer the softmax activation function is used (Peng et al., 2017) equation 4, this function is responsible for making the probabilistic distribution of the input image belong to each of the classes in which the network was trained. To reduce the training time and to avoid overfitting is used dropout in the layer, ie it is randomly removed at each training interaction, a certain percentage of the neurons of a layer, re-adding them in the following iteration. The loss function used was equation 3 and the optimization function used was ADAM (Kingma and Ba, 2014)

$$\sigma(\mathbf{z})_j = \frac{e^{z_j}}{\sum_{k=1}^K e^{z_k}} \text{ for } j = 1, \dots, K. \quad (4)$$

## 4 METRICS OF THE EVALUATION

### 4.1 Cross Validation

Cross-validation is one of the fundamental methods in machine learning for method evaluation and parameter selection in a machine prediction or learning task. Thus, K-fold cross validation was used to evaluate this model.

In K-fold cross-validation, the sample is randomly divided into  $k$  sets of equal sizes. In each of the  $k$  shares, a single set is separated as the validation data to test the model, and the remaining sets of  $k - 1$  are used as training data (Fan and Hauser, 2018). The cross-validation process is then repeated  $k$  times, with each of the  $k$  sets used exactly once for validation (Fan and Hauser, 2018). The mean performance is then used as the evaluation index of the method studied. This approach can be computationally expensive, but it takes full advantage of the entire set of data, especially when the number of samples is very small (Men et al., 2018). This approach can also demonstrate how the trained model is generalizable for unseen data in order to avoid deliberate choice of data with superior test results (Men et al., 2018).

### 4.2 Confusion Matrix

The confusion matrix is an array that contains correct and incorrect predictions of the algorithm and the actual situation. As shown in table 1.

- True Positive: Number of people who actually have pneumonia according to the algorithm.
- False Negative: Number of people who are actually with pneumonia but categorized as healthy according to the algorithm.

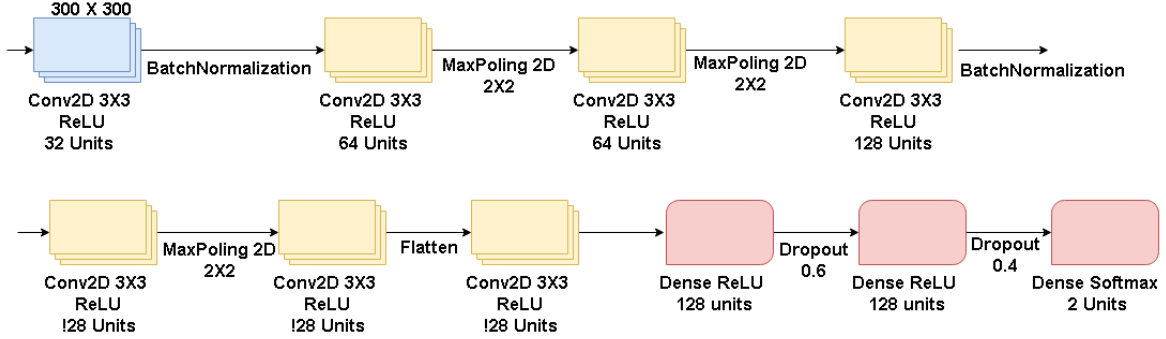


Figure 5: Construction of the CNN training mode.

Table 1: Confusion Matrix.

	<b>Positive Predicted</b>	<b>Negative Predicted</b>
Positive	True Positive	False Negative
Negative	False Positive	True Negative

- False Positive: Number of people who are actually healthy, but categorized as pneumonia, according to the algorithm.
- True Negative: Number of people who are really healthy and categorized as healthy according to the algorithm.

### 4.3 ROC Curve

The ROC curve is a graphical representation that visualizes the relationship between the true positive rate and the false positive rate for a classifier under various decision thresholds. Thus, a ROC curve is conceptually equivalent to a curve that shows the relationship between the power of the test and the probability of error, with the variation of the cutoff value of a statistical test. Therefore, the ROC curve compares classifier performance across the full range of class distributions, offering an assessment, covering a wide range of operating conditions (Brzezinski and Stefanowski, 2017).

ROC curves are an important tool in assessing the uncertainty format, and are a valuable method in characterizing the strengths and weaknesses of diagnostic tests (Junge and Dettori, 2018).

## 5 RESULTS

In this section will be presented the results obtained by the classification model described above. The metrics used reinforce the results, in the table 2 CNN performance results compared to the work of (Kermany

et al., 2018). In Figure 7 you can view a graph with the ROC curve. In the figure 8 the confusion matrix for iteration 1 of the table 2.

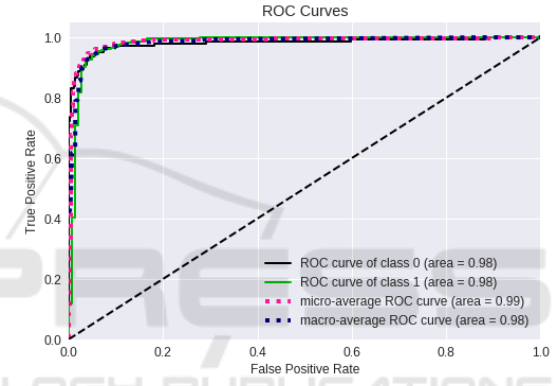


Figure 6: ROC curve interaction 1 reference table 2.

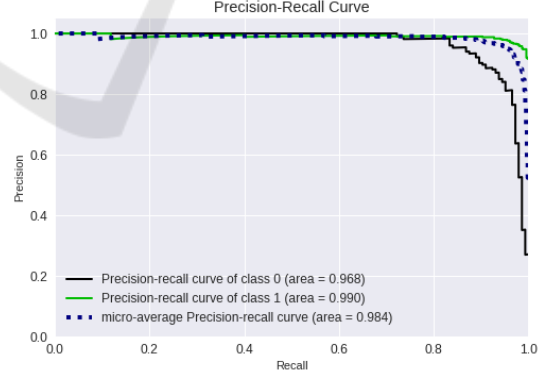


Figure 7: Precision Recall curve interaction 1 reference table 2.

## 6 CONCLUSIONS

In this paper we have demonstrated a comparison with the work of (Kermany et al., 2018) in the detection and classification of images for the detection of pneumonia from the chest X-ray of patients. The Convo-

lutional Neural Network was used to train the neural network and, for the validation of the model, Cross validation was used. The classification model presented was efficient in the classification, obtaining an average accuracy of 95.30 % in the tests against 92.8 % of the work of (Kermany et al., 2018).

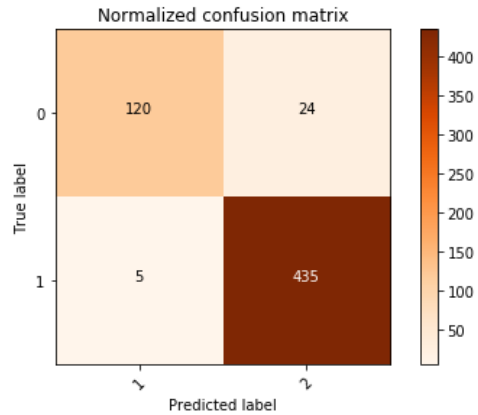


Figure 8: Confusion matrix reference interaction 1 table 2.

Table 2: Accuracy of the interactions the model learning.

**		Normal	Pneumonia	ACC
1	Normal	<b>120</b>	24	
1	Pneumonia	5	<b>435</b>	
1				<b>95.03 %</b>
2	Normal	<b>131</b>	33	
2	Pneumonia	2	<b>418</b>	
2				<b>94.00 %</b>
3	Normal	<b>117</b>	25	
3	Pneumonia	3	<b>439</b>	
3				<b>95.20 %</b>
4	Normal	<b>142</b>	17	
4	Pneumonia	5	<b>420</b>	
4				<b>96.23 %</b>
5	Normal	<b>132</b>	19	
5	Pneumonia	2	<b>431</b>	
5				<b>96.04 %</b>
**	(Kermany et al., 2018)			<b>92.8 %</b>
**	Average accuracy this paper			<b>95.30 %</b>

## ACKNOWLEDGMENTS

This work is financed by National Funds through the FCT - Fundação para a Ciência e a Tecnologia (Portuguese Foundation for Science and Technology) as part of project UID/EEA/00760/2019.

## REFERENCES

- Amrulloh, Y. A., Abeyratne, U. R., Swarnkar, V., Herath, D., Triasih, R., and Setyati, A. (2018). Hmm based cough sound analysis for classifying pneumonia and asthma in pediatric population. In Eskola, H., Väistönen, O., Viik, J., and Hyttinen, J., editors, *EMBEC & NBC 2017*, pages 852–855, Singapore. Springer Singapore.
- Barrientos, R., Roman-Gonzalez, A., Barrientos, F., Solis, L., Correa, M., Pajuelo, M., Anticona, C., Lavarello, R., Castañeda, B., Oberhelman, R., Checkley, W., Gilman, R. H., and Zimic, M. (2016). Automatic detection of pneumonia analyzing ultrasound digital images. In *2016 IEEE 36th Central American and Panama Convention (CONCAPAN XXXVI)*, pages 1–4.
- Brzezinski, D. and Stefanowski, J. (2017). Prequential auc: properties of the area under the roc curve for data streams with concept drift. *Knowledge and Information Systems*, 52(2):531–562.
- Cortellaro, F., Colombo, S., Coen, D., and Duca, P. G. (2012). Lung ultrasound is an accurate diagnostic tool for the diagnosis of pneumonia in the emergency department. *Emergency Medicine Journal*, 29(1):19–23.
- d. Nóbrega, R. V. M., Peixoto, S. A., d. Silva, S. P. P., and Filho, P. P. R. (2018). Lung nodule classification via deep transfer learning in ct lung images. In *2018 IEEE 31st International Symposium on Computer-Based Medical Systems (CBMS)*, pages 244–249.
- Fan, C. and Hauser, H. (2018). Fast and accurate cnn-based brushing in scatterplots. In *Computer Graphics Forum*, volume 37, pages 111–120. Wiley Online Library.
- Junge, M. R. J. and Dettori, J. R. (2018). Roc solid: Receiver operator characteristic (roc) curves as a foundation for better diagnostic tests. *Global Spine Journal*, 8(4):424–429.
- Kermany, D. S., Goldbaum, M., Cai, W., Valentim, C. C., Liang, H., Baxter, S. L., McKeown, A., Yang, G., Wu, X., Yan, F., et al. (2018). Identifying medical diagnoses and treatable diseases by image-based deep learning. *Cell*, 172(5):1122–1131.
- Kermany, Daniel; Zhang, K. G. M. (2018). Labeled optical coherence tomography (oct) and chest x-ray images for classification. *Mendeley Data*.
- Khobragade, S., Tiwari, A., Patil, C. Y., and Narke, V. (2016). Automatic detection of major lung diseases using chest radiographs and classification by feed-forward artificial neural network. In *2016 IEEE 1st International Conference on Power Electronics, Intelligent Control and Energy Systems (ICPEICES)*, pages 1–5.
- Kingma, D. P. and Ba, J. (2014). Adam: A method for stochastic optimization. *CoRR*, abs/1412.6980.
- Lisowska, A., Beveridge, E., Muir, K., and Poole, I. (2017). Thrombus detection in ct brain scans using a convolutional neural network. In *BIOIMAGING*, pages 24–33.
- Mabaso, M. A., Withey, D. J., and Twala, B. (2018). Spot

- detection in microscopy images using convolutional neural network with sliding-window approach.
- Marques, J. F., das Chagas, Fontenele, A. A., Costa, J. V. M., De Araujo, N. F., and Valente, A. (2018). Manipulation of bioinspiration robot with gesture recognition through fractional calculus. *IEEE LARS 2018 – 15th Latin American Robotics Symposium*.
- Mathur, S., Fuchs, A., Bielicki, J., Anker, J. V. D., and Sharland, M. (2018). Antibiotic use for community-acquired pneumonia in neonates and children: Who evidence review. *Paediatrics and International Child Health*, 38(sup1):S66–S75. PMID: 29790844.
- Men, K., Geng, H., Cheng, C., Zhong, H., Huang, M., Fan, Y., Plastaras, J. P., Lin, A., and Xiao, Y. (2018). More accurate and efficient segmentation of organs-at-risk in radiotherapy with convolutional neural networks cascades. *Medical physics*.
- Paing, M. P. and Choomchay, S. (2017). A computer aided diagnosis system for detection of lung nodules from series of ct slices. In *2017 14th International Conference on Electrical Engineering/Electronics, Computer, Telecommunications and Information Technology (ECTI-CON)*, pages 302–305.
- Peng, H., Li, J., Song, Y., and Liu, Y. (2017). Incrementally learning the hierarchical softmax function for neural language models. In *AAAI*, pages 3267–3273.
- Ponzio, F., Macii, E., Ficarra, E., and Di Cataldo, S. (2018). Colorectal cancer classification using deep convolutional networks.
- Rajaraman, S., Candemir, S., Kim, I., Thoma, G., and Antani, S. (2018). Visualization and interpretation of convolutional neural network predictions in detecting pneumonia in pediatric chest radiographs. *Applied Sciences*, 8(10).
- Rizal, A., Hidayat, R., and Nugroho, H. A. (2016). Pulmonary crackle feature extraction using tsallis entropy for automatic lung sound classification. In *2016 1st International Conference on Biomedical Engineering (IBIOMED)*, pages 1–4.
- Rizal, A., Hidayat, R., and Nugroho, H. A. (2017). Entropy measurement as features extraction in automatic lung sound classification. In *2017 International Conference on Control, Electronics, Renewable Energy and Communications (ICCREC)*, pages 93–97.
- Rodrigues, M. B., Nóbrega, R. V. M. D., Alves, S. S. A., Filho, P. P. R., Duarte, J. B. F., Sangaiah, A. K., and Albuquerque, V. H. C. D. (2018). Health of things algorithms for malignancy level classification of lung nodules. *IEEE Access*, 6:18592–18601.
- Santosh, K. C. and Antani, S. (2018). Automated chest x-ray screening: Can lung region symmetry help detect pulmonary abnormalities? *IEEE Transactions on Medical Imaging*, 37(5):1168–1177.
- Saraiva, A., Barros, M., Nogueira, A., Fonseca Ferreira, N., and Valente, A. (2018a). Virtual interactive environment for low-cost treatment of mechanical strabismus and amblyopia. *Information*, 9(7):175.
- Saraiva, A., Miranda de Jesus Castro, F., Ferreira, N., and Valente, A. (2018b). Compression of electrocardiograms comparative study between the walsh hadamard transform and discrete cosine transform.
- Saraiva, A. A., , N. F. F. Salviano F.S.P. Soares and, M. J. C. S. R., and Antonio, V. (2018c). Filtering of cardiac signals with mathematical morphology for qrs detection. *Proceedings of ICAT'18, 7th International Conference on Advanced Technologies*.
- Saraiva, A. A., Costa, N., Sousa, J. V. M., De Araujo, T. P., Ferreira, N. F., and Valente, A. (2018d). Scalable task cleanup assignment for multi-agents. In *Memorias de Congresos UTP*, volume 1, pages 439–446.
- Saraiva, A. A., Ferreira, N. M. F., and Valente, A. (2018e). New bioinspired filter of dicom images. In *Proceedings of the 11th International Joint Conference on Biomedical Engineering Systems and Technologies - Volume 1: BIODEVICES*, pages 258–265. INSTICC, SciTePress.
- Saraiva, A. A., Nogueira, A. T., Ferreira, N. F., and Valente, A. (2018f). Application of virtual reality for the treatment of strabismus and amblyopia. In *2018 IEEE 6th International Conference on Serious Games and Applications for Health (SeGAH)*, pages 1–7. IEEE.
- Saraiva, A. A., SANTOS, D. S., JUNIOR, F. M., SOUSA, J. V. M., FERREIRA, N. F., and Valente, A. (2018g). Navigation of quadruped multirobots by gesture recognition using restricted boltzmann machines. In *Memorias de Congresos UTP*, volume 1, pages 431–438.
- Sharma, A., Raju, D., and Ranjan, S. (2017). Detection of pneumonia clouds in chest x-ray using image processing approach. In *2017 Nirma University International Conference on Engineering (NUiCONE)*, pages 1–4.
- Zar, H. J., Andronikou, S., and Nicol, M. P. (2017). Advances in the diagnosis of pneumonia in children. *BMJ*, 358.
- Zhang, C., Sun, G., Fang, Z., Zhou, P., Pan, P., and Cong, J. (2018). Caffeine: Towards uniformed representation and acceleration for deep convolutional neural networks. *IEEE Transactions on Computer-Aided Design of Integrated Circuits and Systems*, pages 1–1.
- Zhang, Z. and Sabuncu, M. R. (2018). Generalized cross entropy loss for training deep neural networks with noisy labels. *CoRR*, abs/1805.07836.